

RADIATION PRESSURE DRIVEN GALACTIC WINDS FROM SELF-GRAVITATING DISKS

DONG ZHANG¹ & TODD A. THOMPSON^{1,2,3}

SUBMITTED TO APJ:

ABSTRACT

We study large-scale winds driven from uniformly bright self-gravitating disks radiating near the Eddington limit. We show that the ratio of the radiation pressure force to the gravitational force increases with height to a maximum of twice its value at the disk surface. Thus, uniformly bright self-gravitating disks radiating at the Eddington limit are fundamentally unstable to driving large-scale winds. These results contrast with the spherically symmetric case, where super-Eddington luminosities are required for wind formation. We apply this theory to galactic winds from starburst galaxies that approach the Eddington limit for dust. For hydrodynamically coupled gas and dust, we find that the asymptotic velocity of the wind is $v_\infty \simeq 3\langle v_{\text{rot}} \rangle$ and that $v_\infty \propto \text{SFR}^{0.36}$, where $\langle v_{\text{rot}} \rangle$ is the mean disk rotation velocity and SFR is the star formation rate, both of which are in agreement with observations. However, these results of the model neglect the gravitational potential of the surrounding dark matter halo and a (potentially massive) old stellar bulge, which both act to decrease v_∞ . A more realistic treatment shows that the flow can either be unbound, or bound, forming a “fountain flow” with a typical turning timescale of $t_{\text{turn}} \sim 0.1 - 1$ Gyr, depending on the ratio of the mass and radius of the starburst disk relative to the total mass and break (or scale) radius of the dark matter halo or bulge. We provide quantitative criteria and scaling relations for assessing whether or not a starburst of given properties can drive unbound flows via the mechanism described in this paper. Importantly, we note that because t_{turn} is longer than the star formation timescale (gas mass/star formation rate) in the starbursts and ultra-luminous infrared galaxies for which our theory is most applicable, if starbursts are selected as such, they may be observed to have strong outflows along the line of sight with a maximum velocity v_{max} comparable to $\sim 3\langle v_{\text{rot}} \rangle$, even though their winds are in fact bound on large scales.

Subject headings: Galaxies: Starburst — Galaxies: Formation — Galaxies: IGM — Galaxies: Halos

1. INTRODUCTION

Galactic-scale winds are ubiquitous in starburst galaxies in both the local and high-redshift universe (Heckman et al. 1990; Heckman et al. 2000; Pettini et al. 2001, 2002; Shapley et al. 2003; Rupke et al. 2005; Sawicki et al. 2008). They are important for determining the chemical evolution of galaxies and the mass-metallicity relation (Dekel & Silk 1986; Tremonti et al. 2004; Erb et al. 2006; Finlator & Davé 2008; Peeples & Shankar 2011), and as a primary source of metals in the intergalactic medium (IGM; e.g., Aguirre et al. 2001). Moreover, galactic winds are perhaps the most extreme manifestation of the feedback between star formation in a galaxy and its interstellar medium (ISM). This feedback mechanism is crucial for understanding galaxy formation and evolution over cosmic time (Springel & Hernquist 2003; Oppenheimer & Davé 2006; Oppenheimer & Davé 2008; Oppenheimer et al. 2010).

The most well-developed model for galactic winds from starbursts is the supernova-driven model of Chevalier & Clegg (1985), which assumes that the energy from multiple stellar winds and core-collapse supernovae in the starburst is efficiently thermalized. The resulting hot flow drives gas out of the host, sweeping up the cool ISM (Heckman, Lehnert & Armus 1993; Strickland & Stevens 2000; Strickland et al. 2002; Strickland & Heckman 2009; Fujita et al. 2009). Although this model is successful in explaining the X-ray properties of starbursts, the recent

observational results that galaxies with higher star formation rates (SFRs) accelerate the absorbing cold gas clouds to higher velocities ($v \propto \text{SFR}^{0.35}$) and that the wind velocity is correlated with the galaxy escape velocity may challenge the traditional hypothesis that the cool gas is accelerated by the ram pressure of the hot supernova-heated wind, whose X-ray emission temperature varies little with SFR, circular velocity, and host galaxy mass, indicating a critical galaxy mass below which most of the hot wind escapes. These new observations may instead favor momentum-driven or radiation pressure-driven models for the wind physics (e.g., Martin 1999; Martin 2005; Weiner et al. 2009; Murray, Quataert & Thompson 2005 [hereafter MQT05]).

The model that galactic winds may be driven by momentum deposition provided by radiation pressure from the continuum absorption and scattering of starlight on dust grains was developed by MQT05. However, the conclusions of MQT05 are based on an assumed isothermal potential and spherical geometry, and are thus most appropriate for bright elliptical/spheroidal galaxies in formation. On the other hand, the theory of radiation-driven winds from accretion disks from the stellar to galactic scales has also been studied (e.g., Tajima & Fukue 1996, 1998; Proga, Stone & Drew 1998, 1999; Proga 2000, 2003), but none of these works considered radiation from self-gravitating disks.

In this paper we answer the question of whether or not large-scale winds can be driven by radiation pressure from self-gravitating disks radiating near the Eddington limit. These considerations are motivated by the work of Thompson, Quataert & Murray (2005; TQM05), who argued that radiation pressure on dust is the dominant feedback mechanism in starbursts, and that in these systems star formation

¹ Department of Astronomy, The Ohio State University, 140 W. 18th Ave., Columbus, OH, 43210; dzhang, thompson@astronomy.ohio-state.edu

² Center for Cosmology & Astro-Particle Physics, The Ohio State University, 191 West Woodruff Ave., Columbus, OH, 43210

³ Alfred P. Sloan Fellow

is Eddington-limited. For simplicity, throughout this paper we assume that the disk is of uniform brightness and surface density. In §2, we show that such disks are fundamentally unstable to wind formation because the radiation pressure force dominates gravity in the vertical direction above the disk surface. This result is qualitatively different from the well-known case in spherical symmetry. In §2, we also discuss the applicability of this model to starbursts and then calculate the terminal velocity of the wind along the disk pole, and its dependence on both the SFR and galaxy escape velocity. In §3, we assess the importance of a spherical stellar bulge and dark matter halo potential. In §4, we discuss the 3-dimensional wind structure and estimate the total wind mass loss rate. We discuss our findings and conclude in §5.

2. RADIATION-DRIVEN WINDS & THE TERMINAL VELOCITY

We consider a disk with uniform brightness and total surface density: $I(r \leq r_{\text{rad}}) = I$ and $\Sigma(r \leq r_D) = \Sigma$, where r_{rad} and r_D define the outer radius of the luminous and gravitating portion of the disk, respectively. The flux-mean opacity to absorption and scattering of photons is κ . The gravitational force along the polar axis above the disk is

$$\begin{aligned} f_{\text{grav}}(z) &= -2\pi G \Sigma \int_0^{r_D} \frac{z r dr}{(r^2 + z^2)^{3/2}} \\ &= -2\pi G \Sigma \left(1 - \frac{z}{\sqrt{z^2 + r_D^2}} \right), \end{aligned} \quad (1)$$

and the vertical radiation force along the pole is (e.g., Proga, Stone & Drew 1998; Tajima & Fukue 1998)

$$f_{\text{rad}}(z) = \frac{2\pi \kappa I}{c} \int_0^{r_{\text{rad}}} \frac{z^2 r dr}{(r^2 + z^2)^2} = \frac{\pi \kappa I}{c} \frac{r_{\text{rad}}^2}{z^2 + r_{\text{rad}}^2}. \quad (2)$$

The extra factor $z/\sqrt{r^2 + z^2}$ in the radiation force integral compared with the gravitational force makes the Eddington ratio along the pole $\Gamma(z) = |f_{\text{rad}}(z)/f_{\text{grav}}(z)|$ a function of height z

$$\Gamma(z) = \Gamma_0 \left(\frac{r_{\text{rad}}}{r_D} \right)^2 \left(\frac{z^2 + r_D^2}{z^2 + r_{\text{rad}}^2} + \frac{z\sqrt{z^2 + r_D^2}}{z^2 + r_{\text{rad}}^2} \right), \quad (3)$$

where $\Gamma_0 = \Gamma(z=0) = \kappa I/(2cG\Sigma)$ is the Eddington ratio at the disk center. A disk at the Eddington limit ($\Gamma_0 = 1$) requires $I_{\text{Edd}} = 2cG\Sigma/\kappa$, or flux $F_{\text{Edd}} = 2\pi cG\Sigma/\kappa$. If $r_{\text{rad}}/r_D > 1/\sqrt{2} \simeq 0.7$, then $\Gamma(z)$ increases along the z -axis above the disk. In particular, for $r_{\text{rad}} \simeq r_D$, the radiation force becomes twice the gravitational force as $z \rightarrow \infty$:

$$\Gamma_\infty = \Gamma(z \rightarrow \infty) = 2. \quad (4)$$

Because $\Gamma(z)$ increases monotonically with z , an infinitesimal displacement of a test particle in the vertical direction yields a net vertical acceleration, and the disk is thus unstable to wind formation. This result for disks is qualitatively different from the spherical case with a central point source where $\Gamma = f_{\text{rad}}/f_{\text{grav}}$ is constant with radius.

If we consider the motion of a test particle in the outflow, the velocity along the z -axis can be written as

$$\frac{v(z)^2 - v_0^2}{4\pi G \Sigma r_D} = \hat{r} \Gamma_0 \arctan \left(\frac{\hat{z}}{\hat{r}} \right) - \left(1 + \hat{z} - \sqrt{1 + \hat{z}^2} \right), \quad (5)$$

where $\hat{r} = r_{\text{rad}}/r_D$, $\hat{z} = z/r_D$, and v_0 is initial vertical velocity. The first term on the right side of equation (5) is the ‘‘radiation potential’’ along the pole, while the second term is the

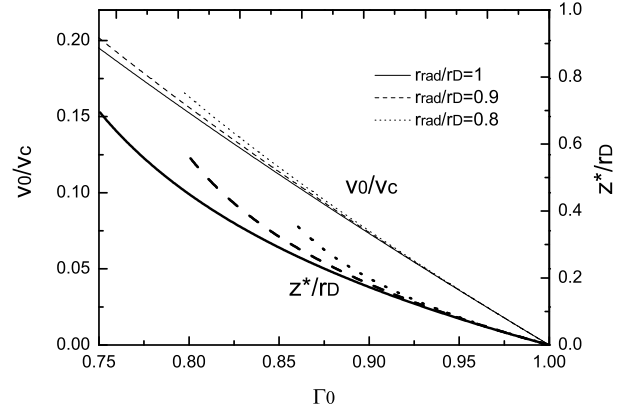


FIG. 1.— Minimum initial velocity v_0/v_c to drive unbound winds (thin lines), and the critical height z^* turning the gas from deceleration to accelerations (thick lines) as a function of Eddington ratio Γ_0 in the sub-Eddington case $2/(\pi \hat{r}) < \Gamma_0 < 1$, where $\hat{r} = r_{\text{rad}}/r_D = 1, 0.9$ and 0.8 .

gravitational potential. The right side is always positive if $\Gamma_0 \geq 1$ and $\hat{r}\Gamma_0 > 2/\pi \approx 0.64$, and thus the gas can be accelerated to infinity. On the other hand, an unbound outflow is still possible in the sub-Eddington case $\Gamma_0 < 1$ if the initial velocity v_0 is sufficiently large to escape the gravitational potential above the disk until reaching the critical height z^* where $\Gamma(z^*) = 1$, because the gas is decelerated from its initial v_0 until it reaches z^* , it will be accelerated to infinity if $v(z^*) \geq 0$. Using this constraint we calculate the minimum v_0 required to drive an unbound wind in the sub-Eddington case, and the critical height z^* where the wind profile acceleration changes sign. Figure 1 shows the results. We introduce a characteristic velocity $v_c = \sqrt{4\pi G \Sigma r_D}$. The calculation is applied for $v_\infty = v(z \rightarrow \infty) \geq v_0$, or $\hat{r}\Gamma_0 > 2/\pi \simeq 0.64$. In this case the wind can be finally accelerated at infinity. The important point here is that for a disk with sub-Eddington brightness, and non-zero vertical velocity v_0 , the gas can be first decelerated and then accelerated to infinity. For the typical random initial velocities of gas in galaxies $\rho v_0^2 \sim \pi G \Sigma^2$, we have $v_0/v_c \sim (h/2r_D)^{1/2} \sim 0.22(r/r_D)^{1/2}$, where the galactic thickness scale $h = 0.1r$ has been assumed for the second equality (Downes & Solomon 1998). For this reason we expect that even somewhat sub-Eddington disks can drive outflows, as shown in Figure 1. In contrast with the spherical case for which $v_\infty^2 - v_0^2 \propto \Gamma_0 - 1$, uniformly bright self-gravitating disks allow the gas above the disk to be accelerated for the case with $\Gamma_0 = 1$ or even for some sub-Eddington cases. In §4, we show the 3-dimensional trajectories of wind particles launched from both Eddington and sub-Eddington disks.

We wish to apply this simple theory to starburst galaxies, which may reach the Eddington limit for dust (TQM05). However, this application depends on the extent to which a disk-like collection of point sources of radiation (stars) may be treated as a uniformly bright disk. In the limit that the dusty gas of starbursts is optically-thick to the re-radiated FIR emission ($\Sigma \gtrsim 0.1 - 1 \text{ g cm}^{-2}$; $\kappa_{\text{FIR}} \sim 1 - 10 \text{ cm}^2 \text{ g}^{-1}$; see TQM05), as is reached in ULIRGs, the self-gravitating disks around bright AGN, and some starbursts, the approximation of a uniform brightness disk is likely valid. However, for $\Sigma \lesssim 10^{-3} \text{ g cm}^{-2}$ ($\kappa_{\text{UV}} \sim 10^3 \text{ cm}^2 \text{ g}^{-1}$) the disk is optically thin to the UV radiation of massive stars and the approximations of this paper are invalidated. In the intermediate

regime $10^{-3} \lesssim \Sigma \lesssim 0.1 - 1 \text{ g cm}^{-2}$,⁴ the disk is optically-thick to UV radiation, but optically-thin to the re-radiated FIR (the so-called “single-scattering” limit), the application of the simple uniformly bright disk model is tentative, as it depends on the distribution of the sources relative to the dusty gas, the inter-star spacing relative to the vertical scale of the dusty gas, and the grain size distribution, which affects the overall scattering albedo. We save a detailed investigation to a future work, but here note two important points: (1) even for low- Σ galaxies, the fraction of diffuse (potentially scattered) UV light may be substantial (Thilker et al. 2005), and (2) if a finite thickness disk radiates at the single-scattering Eddington limit (i.e., all photons are scattered/absorbed once in the wind; e.g., MQT05), and if the disk is uniformly emissive and absorptive, then, for example, $\kappa_{\text{UV}} F_{\text{UV}} \sim \kappa_{\text{UV}} F_{\text{tot}} / \tau_{\text{UV}} \sim F_{\text{tot}} / \Sigma > \kappa_{\text{FIR}} F_{\text{FIR}}$, where $\tau_{\text{UV}} \sim \kappa_{\text{UV}} \Sigma$ and F_{tot} , F_{UV} , and F_{FIR} are the total, UV, and FIR fluxes, respectively. The radiation pressure is thus dominated by UV emission from the “skin” of the disk (the $\tau_{\text{UV}} \sim 1$ surface), and $F_{\text{UV}} \sim F_{\text{Edd,UV}} \simeq 2\pi c G \Sigma / \kappa_{\text{UV}}$. A similar argument can be made for all other wavebands that are “single-scattering”.

To proceed with our application to starbursts, the characteristic velocity v_c is written as

$$v_c = \sqrt{4\pi G \Sigma r_D} = 500 \text{ km s}^{-1} \Sigma_0^{1/2} r_{D,1\text{kpc}}^{1/2}, \quad (6)$$

where we take $\Sigma_0 = \Sigma / 1 \text{ g cm}^{-2} = \Sigma / (4800 \text{ M}_{\odot} \text{ pc}^{-2})$, and $r_{D,1\text{kpc}} = r_D / 1 \text{ kpc}$. Momentarily neglecting the importance of the surrounding dark matter halo and the potentially massive old stellar bulge (both of which we evaluate in §3), from equation (5) with $\Gamma_0 = 1$ and $r_{\text{rad}} \simeq r_D$, the asymptotic terminal velocity along the pole is

$$v_{\infty} = v_c \sqrt{\pi/2 - 1} \simeq 380 \text{ km s}^{-1} \Sigma_0^{1/2} r_{D,1\text{kpc}}^{1/2}. \quad (7)$$

This expression for v_{∞} can be related to the star formation rate (SFR) using the Schmidt law, which relates the star formation surface density and gas surface density in galactic disks: $\Sigma_{\text{SFR}} \propto \Sigma_{\text{gas}}^{1.4}$ (Kennicutt 1998). We approximate $\Sigma_{\text{gas}} = 0.5 f_{g,0.5} \Sigma$, where f_g is the gas fraction. Since $\text{SFR} \sim \Sigma_{\text{SFR}} \pi r_D^2$, we have $v_{\infty} \propto \Sigma^{1/2} r_D^{1/2} \propto \Sigma_{\text{gas}}^{1/2} r_D^{1/2} \propto \text{SFR}^{0.36} r_{D,1\text{kpc}}^{-0.21}$ or

$$v_{\infty} \sim 400 \text{ km s}^{-1} f_{g,0.5}^{-0.5} \left(\frac{\text{SFR}}{50 \text{ M}_{\odot} \text{ yr}^{-1}} \right)^{0.36} r_{D,1\text{kpc}}^{-0.21}, \quad (8)$$

which is consistent with the observation $v_{\infty} \propto \text{SFR}^{0.35 \pm 0.06}$ in low-redshift ULIRGs (Martin 2005) and $v_{\infty} \propto \text{SFR}^{0.3}$ for high-stellar-mass and high-SFR galaxies at redshift $z \sim 1$ (Weiner et al. 2009; but, see Fig. 17 from Chen et al. 2010). The observed scatter at a given SFR may be caused by different r_D , f_g , r_{rad}/r_D , v_0 , bulge and dark matter halo mass and the time dependence of wind fountain with the evolution of the stellar population (see §3). Since we only use a simplified uniform disk model to derive equations (7) and (8), a more definitive comparison with the data should await a model with realistic distributions of surface density, opacity, and brightness.

If we assume the galactic disk is in radial centrifugal balance with a Keplerian velocity $v_{\text{rot}} \sim \sqrt{G \Sigma r}$, and we take the typical terminal velocity from equation (7) to compare to the mean rotation velocity as half of that at the radius r_D , we have

$$v_{\infty} \simeq 4 \sqrt{\pi/2 - 1} \langle v_{\text{rot}} \rangle \simeq 3 \langle v_{\text{rot}} \rangle. \quad (9)$$

⁴ These bounds on Σ depend linearly on the gas-to-dust ratio.

This estimate is again made in the absence of galactic bulge and dark matter halo. That the terminal velocity of the wind increases linearly with the galactic rotation velocity is also consistent with the observational results in Martin (2005, Fig 7). Moreover, in their cosmological simulations of structure formation and IGM enrichment by galactic winds, Oppenheimer & Davé (2006) assumed $v_{\infty} = 3\sigma\sqrt{\Gamma_0 - 1} \sim 3\sigma$, where σ is the galactic velocity dispersion (see also Oppenheimer & Davé 2008; Oppenheimer et al. 2010) with the factor of 3 as an assumption essentially putting in by hand. Our equation (9) shows that it can be derived consistently if the wind is driven by radiation pressure from a self-gravitating disk radiating at or near the Eddington limit. However, as we will show in §3, the gravitational potential of the dark matter halo or a spherical old stellar bulge decreases the factor “3” in equation (9) to $\sim 1 - 3$, and can even lead to bound fountain flows. Thus, the factor of 3 in equation (9) cannot be strictly obtained by the mechanism explored in this paper since all starburst galaxies have dark matter halos. Nevertheless, equations (7) - (9) are essential for developing an understanding of the maximum envelope of values for v_{∞} , and its dependence on the observed properties of starbursts. More physics of v_{∞} and its z -dependence is presented in §3.

Finally, we note that the characteristic timescale for the wind to reach its asymptotic velocity is

$$t_c \sim \sqrt{r_D / (4G\Sigma)} \sim 3.5 \times 10^6 \Sigma_0^{-1/2} r_{D,1\text{kpc}}^{1/2} \text{ yr}, \quad (10)$$

which can be compared with the timescale of a bright star-forming disk: $t_{\star} \sim M_{\text{gas}} / \text{SFR}$. Again employing the Schmidt Law, we find that

$$t_{\star} \sim 2 \times 10^8 f_{g,0.5}^{-0.4} \Sigma_0^{-0.4} \text{ yr} \quad (11)$$

or $t_c/t_{\star} \sim 0.02 r_{D,1\text{kpc}}^{1/2} f_{g,0.5}^{0.4} \Sigma_0^{-0.1}$. Therefore, the wind can be accelerated to $\sim v_{\infty}$ before the gas supply is depleted by star formation.⁵

3. BULGE AND DARK MATTER HALO

The galactic bulge and dark matter halo around the galactic disk are important to the wind dynamics. If we do not consider the luminosity from the galactic bulge,⁶ both the bulge and halo only act to decrease the asymptotic wind velocity, and may even cause the wind to fall back to the disk as a “fountain flow”. For the galactic bulge we employ a truncated constant density sphere, and we adopt the NFW potential (Navarro, Frenk & White 1996) to describe the dark matter halo distribution $\rho_{\text{DM}}(r) \propto R^{-1}(R + r_s)^{-3}$, where r_s is the scale radius and $R = \sqrt{r^2 + z^2}$ is the distance to the halo center. For simplicity, in this section we take $r_{\text{rad}} \simeq r_D$. The Eddington limit $\Gamma_0 = 1$ including the dark matter halo becomes

$$\frac{\pi \kappa I}{c} = 2\pi G \Sigma + \frac{1}{2} \frac{GM_{\text{halo}}}{r_s^2 f(c_{\text{vir}})} = 2\pi G \Sigma \left(1 + \frac{f_h}{2c'} \right), \quad (12)$$

where $c_{\text{vir}} = r_{\text{vir}}/r_s$, r_{vir} is the virial radius, $f(c_{\text{vir}}) = \ln(1 + c_{\text{vir}}) - c_{\text{vir}}/(1 + c_{\text{vir}})$, and

$$f_h = \frac{M_{\text{halo}}}{2\pi r_s r_D \Sigma f(c_{\text{vir}})} \sim \frac{M_{\text{halo}}}{2M_{\text{disk}}} \left(\frac{r_D}{r_s} \right) \frac{1}{f(c_{\text{vir}})}. \quad (13)$$

⁵ For an instantaneous burst of star formation, the bolometric luminosity decreases on a timescale $t_{\text{MS}} \sim 4 \times 10^6 \text{ yr}$, the main sequence lifetime of the most massive stars. Comparing with equation (10) we see that $t_c \lesssim t_{\text{MS}}$ only when $\Sigma/r \gtrsim 3 \times 10^9 \text{ M}_{\odot} \text{ kpc}^{-3}$.

⁶ The case of a bright spherical bulge was considered in MQT05.

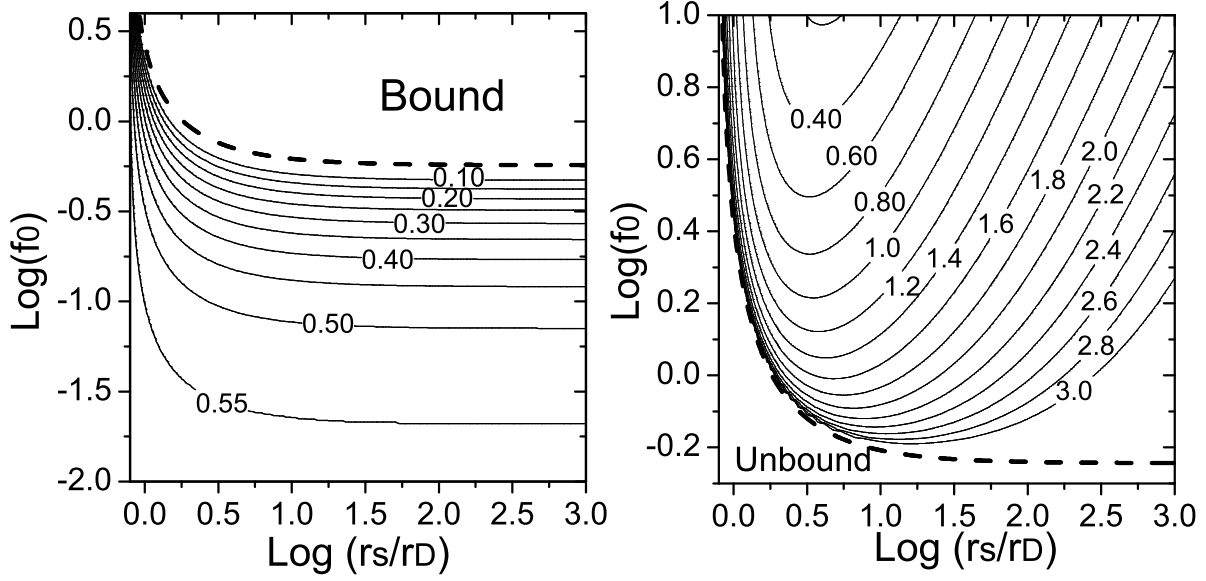


FIG. 2.— Contours of the asymptotic kinetic energy $(v_\infty/v_c)^2$ as a function of $f_0 = f_b + f_h$ (assuming $f_b = 0$) and $c' = r_s/r_D$ for unbound particles (left), and the turning point $\log_{10}(z_{\text{turn}}/r_D)$ along the pole in the case of bound particles, assuming $v_0 = 0$ (right). The dashed line in both panels divides “bound” and “unbound” trajectories.

We introduce the parameters $c' = r_s/r_D$ and

$$f_b = \frac{1}{2} \left(\frac{M_{\text{bulge}}}{M_{\text{disk}}} \right) \left(\frac{r_D}{r_{\text{bulge}}} \right). \quad (14)$$

The parameters f_h and f_b measure the importance of the halo and bulge, respectively, in determining the dynamics of the flow. The asymptotic velocity in terms of these parameters is (see eq. 5)

$$\frac{v_\infty^2 - v_0^2}{v_c^2} = \Gamma_0 \left(1 + \frac{f_h}{2c'} \right) \frac{\pi}{2} - (1 + f_b + f_h). \quad (15)$$

Note that for $f_b, f_h \rightarrow 0$, equations (15) and (7) are equivalent.

We combine the effects of the galactic bulge and dark matter halo using the parameter $f_0 = f_h + f_b$. Assuming $\Gamma_0 = 1$, the condition for matter to be unbound is

$$f_0 < \left[\left(\frac{v_0}{v_c} \right)^2 + \left(\frac{\pi}{2} - 1 \right) \right] \left(1 - \frac{\pi}{4c'} \right)^{-1} \quad (16)$$

For 1 kpc-sized disk and a typical dark matter halo $c' = r_s/r_D \sim 10 - 50$ kpc/1 kpc $\sim 10 - 50$ (Merritt et al. 2006), and an unbound wind for such a disk with $\Gamma_0 = 1$ requires $f_0 \leq 0.6 + (v_0/v_c)^2$.

What is a typical value for f_0 ? If we assume a galaxy with negligible bulge ($f_b \ll f_h$), then

$$f_0 \sim 0.25 \left(\frac{M_{\text{halo}}/M_{\text{disk}}}{30} \right) \left(\frac{r_D/r_s}{1/30} \right) \left(\frac{2}{f(c_{\text{vir}})} \right), \quad (17)$$

where we have taken representative values of $M_{\text{halo}}/M_{\text{disk}} \sim 10 - 100$ (e.g., Leauthaud et al. 2011), $c' = r_s/r_D \sim 10 - 100$, and $f(c_{\text{vir}}) \sim 2$ (for $c_{\text{vir}} \sim 15$; Maccio et al. 2008). We find that for a realistic range of parameters, f_0 is less than ~ 0.6 (eq. 16), which shows that matter accelerated by radiation

pressure may be unbound in many cases. For ultra-luminous infrared galaxies like Arp 220, with physical sizes of order ~ 100 pc (e.g., Downes & Solomon 1998), the factor $c' = r_s/r_D$ may be as large as $\sim 10^3$. However, the ratio of the star-forming disk mass to the total halo mass may be $M_{\text{disk}}/M_{\text{halo}} \sim 10^{-3}$, so that f_h is again ~ 0.3 , potentially implying that in very bright systems outflows can be driven by radiation pressure via the mechanism described here. As equation (13) shows, larger f_0 corresponds to larger r_D , or smaller M_{disk} , for a fixed dark matter halo.

More generally, taking f_0 as a parameter, the terminal velocity from equation (15) is less than the value from equation (7) by a factor

$$\mathcal{D} = \left[1 - \left(\frac{\pi}{2} - 1 \right)^{-1} \left(1 - \frac{\pi}{4c'} \right) f_0 \right]^{1/2}. \quad (18)$$

As a result, both equations (8) and (9) in §2 need to be multiplied by \mathcal{D} when the halo or bulge potential is included. For the purposes of an estimate, taking $c' \sim 10$, the relation between v_∞ and $\langle v_{\text{rot}} \rangle$ becomes

$$v_\infty \simeq 3(1 - 1.6f_0)^{1/2} \langle v_{\text{rot}} \rangle, \quad (19)$$

which shows that the dark matter halo potential well is too deep for particles to escape for $f_0 \gtrsim 0.6$. For $f_0 \simeq 0.25$ in equation (17), instead of the naive estimate without the dark matter halo in equation (9), which yields $v_\infty \simeq 3\langle v_{\text{rot}} \rangle$, we obtain $v_\infty \simeq 2\langle v_{\text{rot}} \rangle$. Even so, equation (19) makes it clear that the factor of 3 in the relation $v_\infty \simeq 3\langle v_{\text{rot}} \rangle$ assumed in the calculation by Oppenheimer & Davé (2006) (see discussion after eq. 9) cannot be strictly achieved for Eddington-limited starbursts by the mechanism discussed in this paper since all systems have dark matter halos, and thus non-zero f_0 . To the extent that the “3” is required by Oppenheimer & Davé (2006),

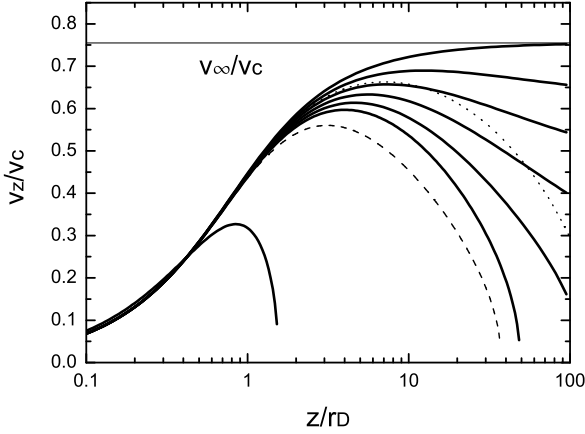


FIG. 3.— Outflow velocity v_z/v_c along the pole with $c' = 10$ and f_0 from top down $f_0 = 0, 0.2, 0.4, 0.6, 0.8, 1, 5$ (thick lines), $c' = 4$ (dashed line) and $c' = 100$ (dotted line) with $f_0 = 1$. The horizon line labeled as v_∞/v_c is the analytical solution as in equation (7).

additional physics such as an effectively super-Eddington galaxy luminosity, supernova-driven hot flows, or the mechanism discussed in Murray, Menard, & Thompson (2011) would be necessary to add to the models here.

The quantitative scaling relations for bound and unbound outflows, encapsulated in the factors f_0 and c' , are illustrated in Figure 2. The left panel shows contours of the asymptotic kinetic energy $(v_\infty/v_c)^2$ as a function of f_0 and $c' = r_s/r_D$ assuming $v_0 = 0$ for unbound outflows.⁷ The right panel of Figure 2 shows contours of $\log_{10}[z_{\text{turn}}/r_D]$, the turning point of the wind scaled to the disk radius for bound “outflows.” All else being equal, a disk with a more massive dark matter halo has larger f_0 , smaller z_{turn} , and the flow has a shorter timescale for reaching the turning point $t_{\text{turn}} \sim z_{\text{turn}}/v_c \sim t_c(z_{\text{turn}}/r_D)$ (see eq. 10). The right panel of Figure 2 shows that z_{turn}/r_D can be larger than 10^3 , implying that the flow reaches many tens of kpc in height above the disk before falling back towards the host on a timescale of $\sim \text{Gyr}$.

Importantly, even if f_0 is large enough that the flow is bound, one may still observe an outgoing wind from a starburst galaxy for two reasons. First, there is a region of parameter space where the time to reach the turning point t_{turn} is larger than the time for the starburst to deplete its gas supply $t_* = M_g/\text{SFR}$ (see eq. 11). Since $t_{\text{turn}}/t_* \sim (z_{\text{turn}}/r_D)t_c/t_*$ (see eq. 10), $z_{\text{turn}}/r_D \gtrsim 60 r_{D,1\text{kpc}}^{-1/2} f_{g,0.5}^{-0.4} \Sigma_0^{0.1}$ is required for $t_{\text{turn}}/t_* \gtrsim 1$. Second, an observable flow along the line of sight to a non-edge-on disk can have a maximum velocity v_{max} that is comparable to v_∞ in equation (7), even though the flow is bound on large scales (z_{turn}) by the dark matter halo. Figure 3 shows the one-dimensional outflow velocity v_z/v_c along the pole with various f_0 and c' . In the bound case, the maximum outflow velocities v_{max} peak around $1-10 r_D$ before decreasing to much lower values. The maximum v_{max} is still comparable to v_∞ in the absence of a halo or bulge, except for very large $f_0 \gtrsim 5$ (see eq. 17). The velocity of the flow before changing sign and falling back to the host galaxy is time-dependent and approximately reaches its maximum at a time $\sim t_c$ (eq. 10).

⁷ Increasing v_0 to $0.2v_c$ does not change the position of the contours appreciably.

The fact that $t_{\text{turn}} > t_*$ and that v_{max} approaches a few $\times \langle v_{\text{rot}} \rangle$ together imply that if galaxies are selected as bright starbursts, they may appear to have unbound outflows even though the gas is in fact bound on large scales by the dark matter halo potential. Indeed, Figure 3 implies that starbursts with bound flows may exhibit a rough correlation of the form $v_{\text{max}} \sim 1-3 \langle v_{\text{rot}} \rangle$.

4. 3-DIMENSIONAL WINDS AND MASS LOSS RATE

So far we have focused on the forces along the polar z -axis. Figure 4 shows 2-dimensional (2D) projections of the 3D orbits of test particles accelerated by radiation pressure and gravity, as well as their constant time surfaces above a uniform disk, starting from an initial height $0.1 r_D$, both with and without an NFW potential, and with no galactic bulge. In the absence of a halo, the upper middle panel shows that winds can be driven even when the disk is sub-Eddington ($\Gamma_0 = 0.88$). The lower panels show that the character of the flow changes significantly as f_0 increases from 0.2, to 0.6, to 1.0 (left to right; compare with eq. 17). For the case $f_0 = 0.2$, the wind is clearly unbound. For $f_0 = 0.6$, particles emerging near the z -axis are accelerated to very large vertical distances, whereas particles emerging from the outer disk region fall back to the disk rapidly. A more massive halo with $f_0 = 1.0$ produces only a “fountain flow” in which particles fall back to the disk with a timescale of $\sim 0.1-1 \text{ Gyr}$. Moreover, Figure 5 gives the 3D orbit vertical component v_z evolution of the particles driven from different disk regions. For the face-on disk, the velocity v_z of the wind is just the velocity along the line of sight. The maximum velocities are reached roughly at $t \sim t_c$. Also, the maximum and terminal velocities of particles from the outer disk region are smaller than those from the inner disk region. As in Figure 4, matter from the outer region of the disk can be bound by the halo’s gravitational potential even though matter from the inner region is unbound.

To estimate the rate of mass ejection from Eddington-limited disks, we first note that the flux and luminosity are

$$F_{\text{Edd}} = 2\pi c G \Sigma / \kappa \sim 3 \times 10^{12} \Sigma_0 \kappa_1^{-1} L_\odot \text{ kpc}^{-2}, \quad (20)$$

and

$$L_{\text{Edd}} = \pi r_{\text{rad}}^2 F_{\text{Edd}} \sim 10^{13} \left(\frac{r_{\text{rad}}}{r_D} \right)^2 \Sigma_0 \kappa_1^{-1} r_{D,1\text{kpc}}^2 L_\odot, \quad (21)$$

respectively, where $\kappa_1 = (\kappa/10) \text{ cm}^2 \text{ g}^{-1}$ is the flux-mean dust opacity. The total mass ejection rate from the disk surface \dot{M}_{ej} is a local quantity measured on a disk scale height, where the gravity of the surrounding bulge and halo is much weaker than the disk’s gravitational and radiation pressure forces (as long as f_0 is not too large). Therefore \dot{M}_{ej} is only determined by the disk, and it can be estimated in the absence of bulge and halo from the integrated momentum equation. In the single-scattering limit, an estimate of \dot{M}_{ej} is

$$\dot{M}_{\text{ej}} v_{\infty, f_0=0} \sim L_{\text{Edd}} / c, \quad (22)$$

where $v_{\infty, f_0=0}$ is the terminal velocity of the flow without a bulge or dark matter halo (eq. 7). Since $v_{\infty, f_0=0}$ is an upper limit to the velocity of the flow (valid as $f_0 \rightarrow 0$; see eq. 19), equation (22) is only approximate. Nevertheless, to the extent that v_{max} is of order $v_{\infty, f_0=0}$ (see Fig. 3), equation (22) should yield an order-of-magnitude estimate of the mass loss rate from the disk itself. Combining equations (7) and (22) we have

$$\dot{M}_{\text{ej}} \sim 3 \times 10^2 \left(\frac{r_{\text{rad}}}{r_D} \right)^2 \Sigma_0^{1/2} \kappa_1^{-1} r_{D,1\text{kpc}}^{3/2} M_\odot \text{ yr}^{-1}, \quad (23)$$

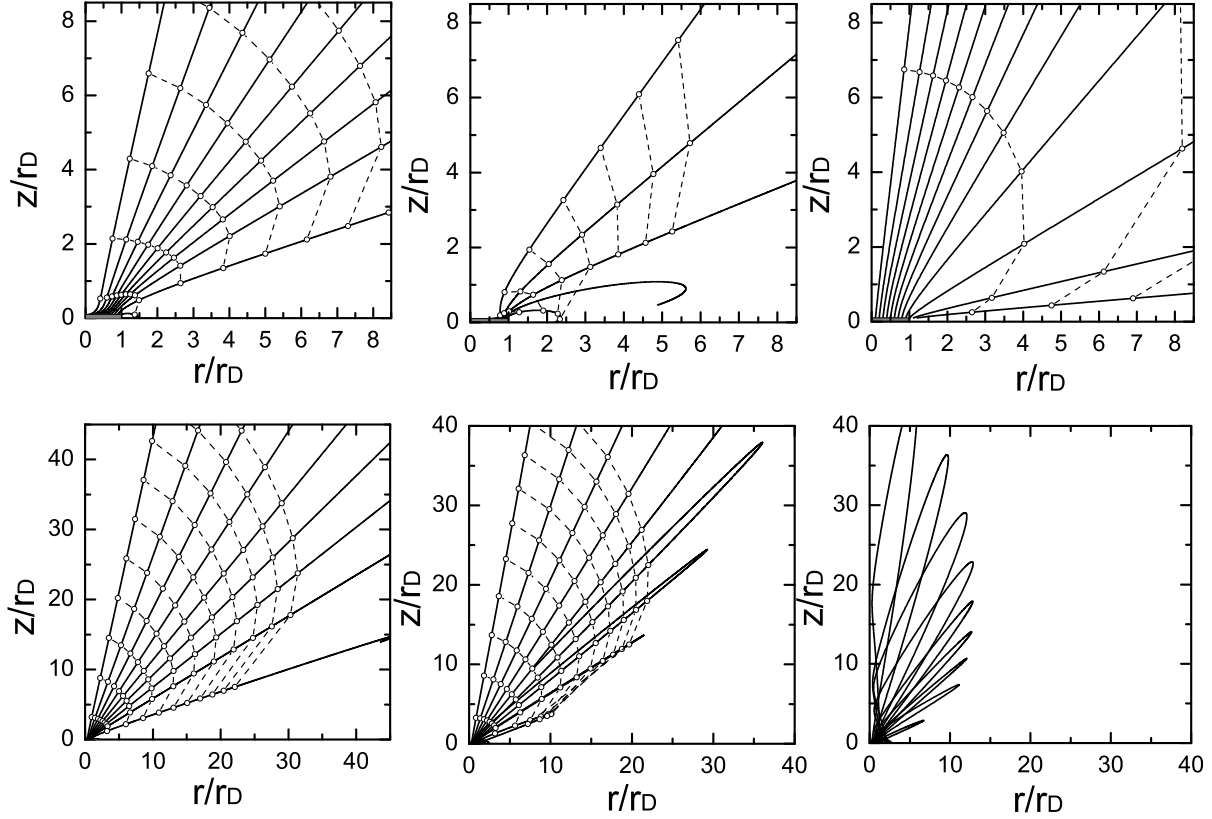


FIG. 4.— The particle orbits from the disk without (upper panels) and with (lower panels) NFW potential. Solid lines show 2-dimensional projections of the 3-dimensional orbits. Upper panels, left to right, we take $\Gamma_0 = 1, 0.88$ and 5 . The particle positions and constant time surfaces are labeled at $t/t_c = 2, 4, 6, 8, 10, \dots$, where $t_c = \sqrt{r_D/(4G\Sigma)}$ (eq. 10). Lower panels, left to right: $f_0 = 0.2, 0.6, 1.0$ with $\Gamma_0 = 1$ and $c' = 10$. Constant time surfaces are marked at $t/t_c = 5, 10, 15, 20, 25, \dots$.

which is similar to observational results (e.g., Martin 2005, 2006). Keep in mind that κ_1 is between the FIR limit $\kappa_{\text{FIR}} \sim 1 - 10 \text{ cm}^2 \text{ g}^{-1}$ and UV limit $\kappa_{\text{UV}} \sim 10^3 \text{ cm}^2 \text{ g}^{-1}$. The estimate for \dot{M}_{ej} thus varies by 2–3 orders of magnitude from FIR-thick to UV-thin disks. Using $L = \epsilon c^2 \text{SFR}$, where $\epsilon_{-3} = \epsilon/10^{-3}$ is an IMF-dependent constant, to calculate the luminosity of a starburst (e.g., Kennicutt 1998), the single-scattering estimate for the ratio of the mass ejection rate to the SFR is

$$\frac{\dot{M}_{\text{ej}}}{\text{SFR}} \sim \frac{\epsilon c}{v_{\infty, f_0=0}} \sim 0.8 \epsilon_{-3} \Sigma_0^{-1/2} r_{D, 1\text{pc}}^{-1/2}, \quad (24)$$

which implies that radiation pressure drives more matter from disks in low-mass galaxies (see MQT05): for example, $\dot{M}_{\text{ej}}/\text{SFR} \gtrsim 10$ for $\Sigma_{r_D} \lesssim 3.1 \times 10^4 M_\odot \text{ pc}^{-1}$. However, as low mass galaxies are usually the most dark matter halo dominated (Persic et al. 1996), with larger f_0 (see eqs. 16 & 17), the matter lost from low mass disks can hardly escape the halo potential, and will fall back on the timescale t_{turn} (see the right panel of Fig. 2). Otherwise, some additional physical mechanism beyond that described in this paper (e.g., a supernova-heated wind) is needed to unbind it from the halo.

The quantity \dot{M}_{ej} in the above expressions is the rate at which matter is ejected from the disk in either a bound or unbound flow. In the former case, as discussed in §3, the outflow

reaches a maximum outward velocity v_{max} before returning to the disk on a timescale t_{turn} , which in many cases is $> t_*$. In the case of an unbound outflow, \dot{M}_{ej} is a rough estimate for the mass loss rate from the halo as a whole on large scales. As emphasized in §3, the critical parameter determining whether or not the flow is bound or unbound is f_0 (eqs. 16 & 17).

5. CONCLUSIONS & DISCUSSION

In this paper we study the large-scale winds from uniformly bright self-gravitating disks radiating near the Eddington limit. Different from the spherical case, where the Eddington ratio $\Gamma = f_{\text{rad}}/f_{\text{grav}}$ is a constant with distance from the source, for disks Γ increases to a maximum of twice its value at the disk surface (§2). As a result, such disks radiating at (or even somewhat below; see Fig. 1) the Eddington limit are unstable to driving large-scale winds by radiation pressure.

We quantify the characteristics of the resulting outflow in the context of Eddington-limited starbursts, motivated by the work of TQM05 who argued that radiation pressure on dust is the dominant feedback process in starburst galaxies. We find that the asymptotic terminal velocity along the polar direction from disks without a stellar bulge or dark matter halo is $v_\infty \sim \sqrt{4\pi G \Sigma r_D} \sim 3 \langle v_{\text{rot}} \rangle$, where r_D is the disk radius, Σ is the surface density, v_{rot} is the disk rotation velocity (see eqs. 7 and 9), and may range from $\sim 50 - 1000 \text{ km s}^{-1}$ for

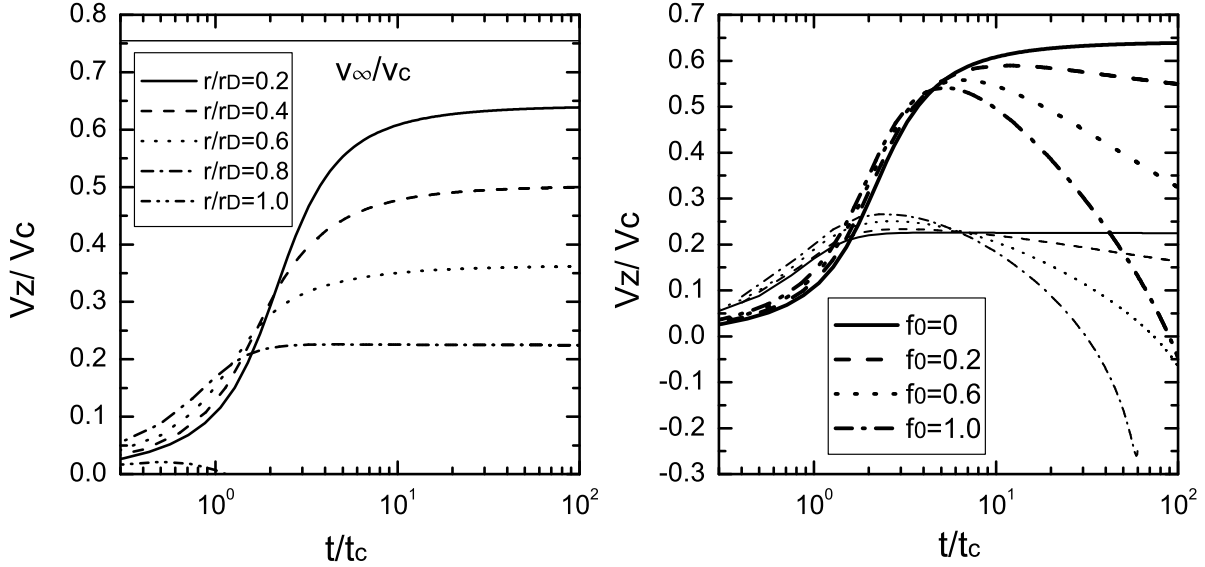


FIG. 5.— *Left panel:* The time evolution of v_z/v_c for $r/r_D = 0.2$ to 1.0 starting with $z/r_D = 0.1$ and $\Gamma_0 = 1$. The horizon line v_∞/v_c is the same as Figure 3. *Right panel:* the velocity v_z/v_c starting from $(r/r_D, z/z_D) = (0.2, 0.1)$ (thick lines) and $(0.8, 0.1)$ (thin lines) with different values f_0 for the dark matter potential with $c' = 10$ and $\Gamma_0 = 1$.

starbursts, depending on the system considered. Furthermore, by employing the observed Schmidt law, we find that $v_\infty \propto \text{SFR}^{0.36} r_D^{-0.21}$ (see eq. 8). These results, in the absence of dark matter halo and bulge, are in agreement with recent observations (e.g., Martin 2005, 2006; Weiner et al. 2009; see also Chen et al. 2010). The typical mass loss rate from an Eddington-limited disk in the single-scattering limit is given by equation (23) and suggests these outflows may efficiently remove mass from the disk (eq. 24).

However, both wind velocities and outflow rates can be significantly decreased by the presence of a spherical old stellar bulge or dark matter halo potential (§3). Deeper or more extended spherical potentials cause the flow to be bound on large scales, and to produce only “fountain flows” where particles fall back to the disk on a typical timescale of $\sim 0.1 - 1$ Gyr, depending on the parameters of the system considered (see Figs. 2-5). The criterion for the flow to become bound is given in equation (16). For typical values of the parameter f_0 (see eq. 17), we find that the winds from starbursts can be either bound or unbound (see Fig. 2). For $f_0 \simeq 0.25$ in equation (17), the asymptotic velocity of the wind is decreased by a factor of $\simeq 0.7$ from the case neglecting the dark matter halo completely (compare eqs. 9 and 19), from $\simeq 3\langle v_{\text{rot}} \rangle$ to $\simeq 2.3\langle v_{\text{rot}} \rangle$. An increase in f_0 by a factor of 2 would decrease the asymptotic velocity further to $\simeq 1.3\langle v_{\text{rot}} \rangle$, whereas an increase of f_0 by a factor of ~ 3 to ~ 0.75 would cause the flow to become bound.

Importantly, even in the limit of bound fountain flows, if the timescale t_{turn} for reaching the turning point z_{turn} is longer than the lifetime of the starburst t_* (eq. 11), one may still observe an outward going wind while the starburst is active and bright. The maximum positive velocity of the flow v_{max} along the line

of sight for non-edge-on disks is still correlated with v_{rot} of the disk (see §3). These facts may complicate the inference from observations of winds that they are unbound from the surrounding large-scale dark matter halo.

Clearly, more detailed work is required to fully assess radiation pressure on dust as the mechanism for launching cool gas from starburst disks. The main limitations of the work presented here are that (1) we consider only disks with constant brightness and surface density, (2) we do not compute the hydrodynamics of the flow, but instead treat the outflow in the test-particle limit, and (3) we ignore other physical effects such as the momentum and energy input from supernovae (Chevalier & Clegg 1985; Strickland & Heckman 2009), which may act in concert with radiation pressure (MQT05; Murray et al. 2010). The general case, with hydrodynamics, realistic disk brightness, surface density, and dust opacity profiles will modify the picture presented here. Such an effort is underway (Zhang & Thompson, in preparation). However, the basic conclusion that uniformly bright self-gravitating disks radiating near the Eddington limit are able to drive large-scale winds — particularly in the high- Σ limit in starbursts (see §2) — should not be fundamentally changed by more elaborate considerations. Indeed, although we have specialized the discussion to starbursts and dust opacity, the instability derived in §2 is of general applicability.

We thank Norman Murray, Crystal Martin, Romeel Davé, the anonymous referee, and especially Mark Krumholz and Eliot Quataert for many stimulating discussions and for a critical reading of the text. This work is supported by NASA grant # NNX10AD01G.

REFERENCES

- Aguirre, A., et al., 2001, *ApJ*, 561, 521
 Chen, Y.-M., et al. 2010, *AJ*, 140, 445
 Chevalier, R. A., & Clegg, A. W. 1985, *Nature*, 317, 44
 Davé, R., Oppenheimer, B. D., & Sivanandam, S. 2008, *MNRAS*, 391, 110

- Dekel, A., & Silk, J. 1986, *ApJ*, 303, 39
- Downes, D., & Solomon, P. M. 1998, *ApJ*, 507, 615
- Erb, D. K., et al. 2006, *ApJ*, 644, 813
- Finlator, K., & Davé, R. 2008, *MNRAS*, 385, 2181
- Fujita, A., et al. 2009, *ApJ*, 698, 693
- Heckman, T. M., Armus, L., & Miley, G. K. 1990, *ApJS*, 74, 833
- Heckman, T. M., Lehnert, M. D., & Armus, L. in Shull, J. M., Thronson, H. A. Jr., eds, *The Environment and Evolution of Galaxies* P. 455 (Kluwer, Dordrecht)
- Heckman, T. M., Lehnert, M. D., Strickland, D. K., & Armus, L., 2000, *ApJ*, 129, 493
- Kennicutt, Jr. R. C. 1998, *ApJ*, 498, 541
- Leauthaud, A. 2011, arXiv: 1104.0928
- Macciò, A. V., et al. 2008, *MNRAS*, 391, 1940
- Martin C. L. 1999, *ApJ*, 513, 156
- Martin C. L. 2005, *ApJ*, 621, 227
- Martin C. L. 2006, *ApJ*, 647, 222
- Merritt, D., Graham, A. W., Moore, B., Diemand, J., & Terzić, B. 2006, *AJ*, 132, 2685
- Murray, N., Quataert, E., & Thompson, T. A. 2005, *ApJ*, 618, 569 (MQT05)
- Murray, N., Ménard, B., & Thompson, T. A. 2010, arXiv:1005.4419
- Navarro, J. F., Frenk, C. S., & White, S. D. M. 1996, *ApJ*, 462, 563
- Oppenheimer, B. D., & Davé, R. 2006, *MNRAS*, 373, 1265
- Oppenheimer, B. D., & Davé, R. 2008, *MNRAS*, 387, 577
- Oppenheimer, B. D., et al. 2010, *MNRAS*, 406, 2325
- Peeples, M. S., & Shankar, F. arXiv: 1007.3743
- Pettini, M., et al. 2001, *ApJ*, 554, 981
- Pettini, M., et al. 2002, *ApJ*, 569, 96
- Persic, M., Salucci, P., & Stel, F. 1996, *MNRAS*, 281, 27
- Proga, D. 2000, *ApJ*, 538, 684
- Proga, D. 2003, *ApJ*, 585, 406
- Proga, D., Stone, J. M., & Drew, J. E. 1998, *MNRAS*, 295, 595
- Proga, D., Stone, J. M., & Drew, J. E. 1999, *MNRAS*, 310, 476
- Rupke, D. S., Veilleux, S., & Sanders, D. B. 2005, *ApJS*, 160, 115
- Sawicki, M., et al. 2008, *ApJ*, 687, 884
- Shapley, A. E., Steidel, C. C., Pettini, M., & Adelberger, K. L. 2003, *ApJ*, 588, 65
- Springel, V., & Hernquist, L. 2003, *MNRAS*, 339, 312
- Strickland, D. K., & Stevens, I. R. *MNRAS*, 2000, 314, 511
- Strickland, D. K., et al. 2002, *ApJ*, 568, 689
- Strickland, D. K., & Heckman, T. M. *ApJ*, 2009, 697, 2030
- Tajima, Y., & Fukue, J. 1996, *PASJ*, 48, 529
- Tajima, Y., & Fukue, J. 1998, *PASJ*, 50, 483
- Thompson, T. A., Quataert, E., & Murray, N. 2005, *ApJ*, 630, 167 (TQM05)
- Thilker, D. A., et al. 2005, *ApJ*, 619, L67
- Tremonti, C. A. et al. 2004, *ApJ*, 613, 898
- Weiner, B. J., et al. 2009, *ApJ*, 692, 187